arXiv:1511.03119v1 [cond-mat.supr-con] 10 Nov 2015

Type-I superconductivity in KBi_2 single crystals

Shanshan Sun[1,2], Kai Liu[1,2], and Hechang Lei[1,2,*]
[1] *Department of Physics, Renmin University of China, Beijing 100872, China*
[2] *Beijing Key Laboratory of Opto-electronic Functional Materials and Micro-nano Devices, Renmin University of China, Beijing 100872, China*

(Dated: November 11, 2015)

We report the detailed transport, magnetic, thermodynamic properties and theoretical calculation of KBi_2 single crystals in superconducting and normal states. KBi_2 shows metallic behavior at normal state and enters superconducting state below $T_c = 3.573$ K. Moreover, KBi_2 exhibits low critical fields in all of measurements, field-induced crossover from second to first-order phase transition in specific heat measurement, typical magnetization isotherms of type-I superconductors, and small Ginzburg-Landau parameter $\kappa_{GL} = 0.611$. These results clearly indicate that KBi_2 is a type-I superconductor with thermodynamic critical field $H_c = 234.3(3)$ Oe.

PACS numbers: 74.25.-q, 74.25.Bt, 74.70.Ad

I. INTRODUCTION

Superconductivity is one of most attractive topics in condensed matter physics area not only because of the great application potential of those superconductors (SCs) with high transition temperature and critical field but also due to the importance of understanding the mechanism of Cooper pairing, especially for the unconventional superconductivity beyond Bardeen-Cooper-Schrieffer (BCS) mechanism. According to the Ginzburg-Landau (GL) theory, the value of GL parameter κ_{GL} which is the ratio of penetration depth to coherence length classifies SCs into two categories: type-I SCs when $\kappa_{GL} < 1/\sqrt{2}$ and type-II SCs when $\kappa_{GL} > 1/\sqrt{2}$.[1] For most of superconducting compounds, they belong to the type-II SCs and have been studied extensively. In contrast, type-I SCs are thought empirically to occur mainly in elementary metals and metalloids and type-I superconducting compounds are very rare.[2] Recently, however, serval binary and ternary compounds are found to be type-I SCs, for instance, $YbSb_2$,[3,4] $TaSi_2$,[5] $LaPd_2Ge_2$,[6] $LaRh_2Si_2$,[7] (Lu, Y, La)Pd_2Si_2,[7] $LaRhSi_3$,[8] $Ag_5Pb_2O_6$,[9] $ScGa_3$ and $LuGa_3$.[10] These studies break the empirical relation between type-I superconductivity and elemental metals and enlarge the family of type-I SCs to binary and ternary compounds.

For the binary bismuth compounds, some of them show superconductivity, such as KBi_2(3.6 K),[11] $SrBi_3$ (5.62 K),[12] $BaBi_3$ (5.69 K),[12] Rh_3Bi_{14} (2.94 K),[13] and In_2Bi (5.9 K).[14] For KBi_2, except superconducting transition temperature T_c, the studies on its physical properties are scarce and its classification of superconductivity has not been identified yet.[11,15] In this work, we performed the detailed characterization and analysis of physical properties for KBi_2 single crystals in superconducting and normal states. Experimental and theoretical calculation results undoubtedly indicate that KBi_2 is a type-I SC in the dirty limit. As far as we know, this is the first type-I SC in the bismuth compounds.

II. EXPERIMENTAL

Single crystals of KBi_2 were grown by the flux method with K : Bi = 1 : 9 molar ratio. K pieces (99.9 %) and Bi shot (99.9 %) were mixed and put into an alumina crucible, covered with quartz wool and then sealed into the quartz tube with partial pressure of Argon. The quartz tube was heated to 580 °C for 12 h and then slowly cooled to 280 °C where crystals were decanted with a centrifuge. Single crystals with typical size 1.8×1.8×1 mm^3 were obtained and exhibit metallic luster. X-ray diffraction (XRD) of powdered small crystals and a single crystal were performed using a Bruker D8 X-ray machine with Cu K_α radiation ($\lambda = 0.15418$ nm) at room temperature. Rietveld refinement of the XRD patterns was performed using the code TOPAS4.[16] Electrical transport, magnetization and specific heat measurements were performed in a Quantum Design PPMS-14. First-principles electronic structure calculations were carried out with the projector augmented wave method[17] as implemented in the VASP package.[18] The generalized gradient approximation of Perdew-Burke-Ernzerh[19] was adopted for the exchange-correlation potential. The kinetic energy cutoff of the plane-wave basis was set to be 350 eV. A supercell containing 2 K atoms and 4 Bi atoms and a $6 \times 6 \times 6$ k-point mesh for the Brillouin zone sampling were employed. The Gaussian smearing with a width of 0.05 eV was used around the Fermi surface. In structure optimization, both cell parameters and internal atomic positions were allowed to relax until the forces were smaller than 0.01 eV/Å. The spin-orbital coupling (SOC) effect was included for the density of states (DOS) calculations.

III. RESULTS AND DISCUSSION

As shown in Fig. 1(a), KBi_2 is isostructural to $MgCu_2$ (Laves phase).[15,20,21] Each unit cell of KBi_2 has 8 K atoms and 16 Bi atoms. Every four Bi atoms form a tetrahedron and these tetrahedra connect each other by vertex-sharing to form a three-dimensional network. K

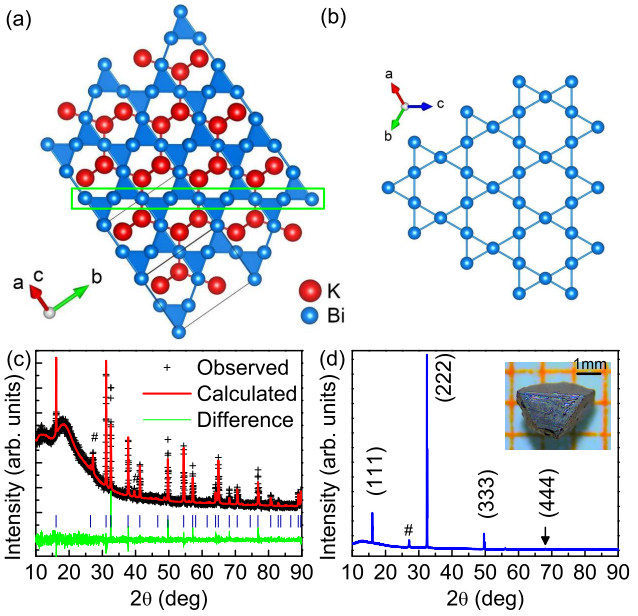

FIG. 1. (a) Crystal structure of KBi_2. The large red and small blue balls represent K and Bi atoms, respectively. The green rectangle marks the (111) plane. (b) The Kagomé net of Bi atoms in (111) plane. (c) Powder XRD pattern of KBi_2. (d) XRD pattern of a KBi_2 single crystal. The extra peaks in XRD patterns (labeled as the # symbol) originate from residual Bi flux. Inset: photo of a typical KBi_2 single crystal. The length of one grid in the photo is 1 mm.

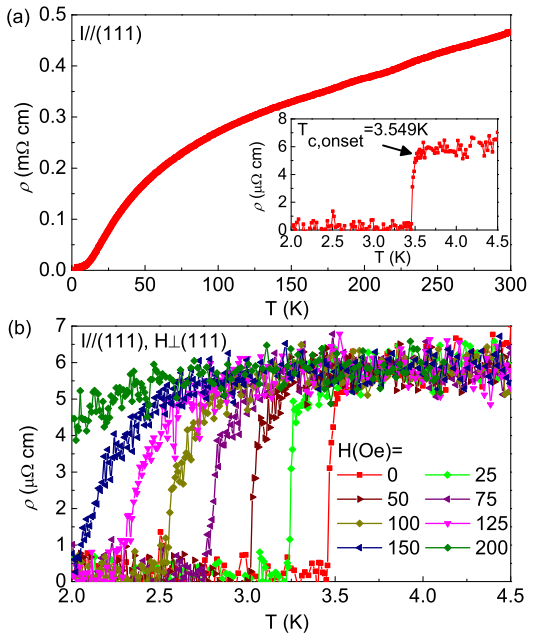

FIG. 2. (a) Temperature dependence of electrical resistivity $\rho(T)$ of KBi_2 single crystal at zero field. Inset: expanded view of the low-temperature data showing the superconducting transition. The $T_{c,onset}$ at zero field is marked by arrow. (b) Low-temperature dependence of $\rho(T)$ of KBi_2 single crystal at various magnetic fields from 0 to 200Oe.

atoms arrange in a diamond lattice which is intertwined with the network of Bi tetrahedra. On the other hand, it can be seen that there are two-dimensional (2D) Kagomé nets of Bi atoms in the (111) plane (Fig. 1(b)), which connect together along [111] direction by other Bi layers, and K atoms locate right above and below the center of hexagons of Bi atoms in the 2D Kagomé nets. The powder XRD pattern of KBi_2 can be well indexed using the $Fd\bar{3}m$ space group ($MgCu_2$-type structure) (Fig. 1(c)). The refined lattice parameters are $a = 0.95233(2)$ nm with $R_p = 5.88$, $R_{wp} = 8.69$ and $\chi^2 = 1.28$, which are close to the values reported in literature ($a = 0.95223(2)$nm).[15] There are some extra peaks that can be ascribed to the diffraction of residual Bi flux. The XRD pattern of a KBi_2 single crystal indicates that the surface of crystal is parallel to the (111) plane (Fig. 1(d)). The KBi_2 crystals prefer to form triangle surface as shown in the inset of Fig.1(d). This characteristic is consistent with the single crystal XRD pattern as well as its crystallographic symmetry.

Fig. 2(a) shows the temperature dependence of electrical resistivity $\rho(T)$ for KBi_2 single crystal at zero field. It can be seen that KBi_2 exhibits metallic behavior and the curve $\rho(T)$ is convex above 25 K, with a tendency to saturate at high temperature. This is a typical shape of resistivity for the sample in which the dominant scattering mechanism is electron-phonon scattering. The residual resistivity ratio (RRR), defined as $\rho(300\ \mathrm{K})/\rho(4\ \mathrm{K})$, is about 72.5, indicating the high quality of single crystal. On the other hand, at zero field, there is a sharp superconducting transition in $\rho(T)$ curve with $T_{c,onset} = 3.549$ K and transition width $\Delta T_c \sim 0.1$ K (inset of Fig. 2(a)). The transition temperature is consistent with previous magnetic susceptibility measurement ($T_c = 3.5$ K).[15] Moreover, with increasing magnetic field, the superconducting transition shifts to lower temperatures gradually and the transition width also becomes wider for $H \perp$ (111) (Fig. 2(b)). Surprisingly, at very low field ($H = 200$ Oe), the T_c has been suppressed below 2 K.

As shown in Fig. 3(a), low-temperature magnetic susceptibility of KBi_2 single crystal for $H \parallel (111)$ with $H = 10$ Oe exhibits diamagnetic signals with sharp transitions appearing at $T_{c,onset} = 3.517$ K ($\Delta T_c = 0.10$ K) for both the zero field cooling (ZFC) and field cooling (FC) modes. This superconducting transition temperature is almost same as that obtained from transport measurement, confirming the superconducting ground state of KBi_2. After considering the demagnetization effect of sample by using the formula $4\pi\chi_{eff} = 4\pi\chi/(1 - N_d\chi)$ where N_d is demagnetization factor and the calculated value is about 0.222,[22] the superconducting volume fraction estimated from the ZFC data is very close to 100 %, indicating that the bulk superconductivity in KBi_2. Meanwhile, the large superconducting volume fraction for FC data suggests the flux pinning effect is rather weak or even absent. Further increasing field suppresses the T_c gradually and when $H = 175$ Oe, the normal states behavior persists down to 2 K, similar to the trend in $\rho(T)$ curves (Fig. 2(b)).

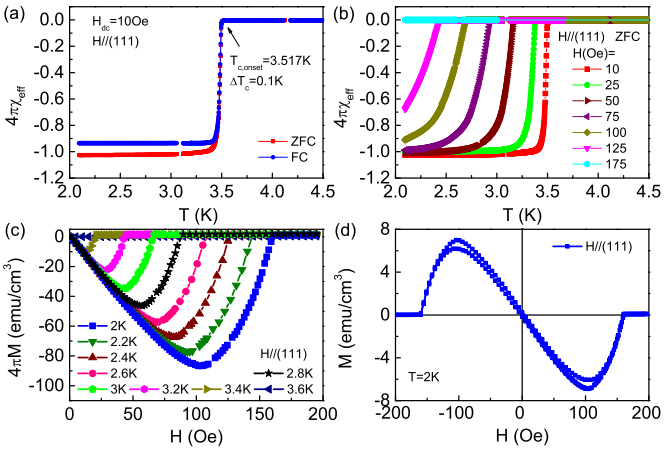

FIG. 3. (a) Temperature dependence of magnetic susceptibility $\chi_{eff}(T) = \chi(T)/(1\text{-}N_d\chi)$ scaled by 4π at $H = 10$ Oe with ZFC and FC modes. The $T_{c,onset}$ is marked by arrow. (b) Temperature dependence of $4\pi\chi_{eff}(T)$ at various magnetic fields with ZFC mode. (c) Low-field parts of $M(H)$ at various temperatures with demagnetization correction.(d) Magnetization loop at $T = 2$ K. For all of measurements, the field direction is parallel to the (111) plane of KBi_2 single crystal.

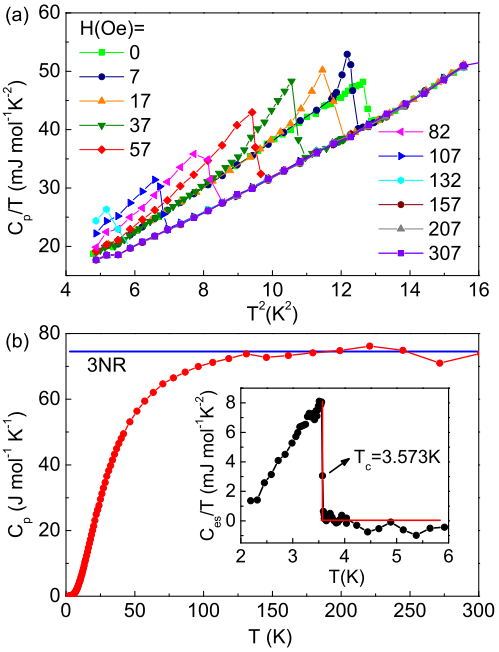

FIG. 4. (a) Low-temperature specific heat C_p/T vs. T^2 of KBi_2 single crystal in a series of magnetic fields from 0 to 307 Oe. (b) Temperature dependence of specific heat from 2.2 K to 300 K at zero field. The solid line shows the classic value of specific heat at high temperature limit. Inset: Temperature dependence of the electronic specific heat plotted as C_{es}/T vs. T at zero field.

Fig. 3(c) shows the dc magnetization isotherms $4\pi M(H)$ of KBi_2 single crystal at various temperatures (from 2 K to 3.6 K) for $H \parallel (111)$ at the low-field range. It can be seen that the magnetic fields corresponding to the maximum absolute values of magnetic moment are very close to those where $4\pi M(H)$ become zero. Based on this, two different assumptions can be made: either (i) KBi_2 is a type-II SC that the upper critical field H_{c2} is very small and close to the lower critical field H_{c1}; or (ii) KBi_2 is a type-I SC and the departure from the ideal step-like transition at critical field may be attributed to a strong pinning of domain walls in the intermediate state or to unclear demagnetization.[23] For the latter case, the critical field H_c is defined as the field where the sample enters to the normal state ($M(H) = 0$). On the other hand, when temperature decreases, the critical field shifts to higher field. Even at the lowest measuring temperature (2 K), however, the critical field is still remarkably small ($\sim$ 160 Oe). The full magnetization loop of KBi_2 measured at 2 K for $H \parallel (111)$ is shown in Fig. 3(d). It can be seen that the hysteresis is very small. The small critical field accompanying with the weak magnetization hysteresis and the shape of $M(H)$ loop similar to other type-I superconducting compounds, such as $YbSb_2$,[3,4] $LaRhSi_3$,[8] $ScGa_3$ and $LuGa_3$,[10] suggest that the KBi_2 is more like a type-I SC rather than a type-II SC.

Specific heats of KBi_2 single crystal at various fields are shown in Fig. 4(a). At zero field, there is a jump at 3.573 K, indicating the bulk superconductivity of KBi_2. The transition temperature is also consistent with the T_c obtained from resistivity and magnetization measurements. More importantly, the specific-heat jump at superconducting transition at $H = 7$ Oe is much sharper and higher than that at zero field, which is a unique feature of type-I SCs and indicates that there is a crossover from second- to first-order phase transition when field is applied. This behavior has been observed in other type-I intermetallic SCs, such as $YbSb_2$,[3,4] $LaRhSi_3$,[8] $ScGa_3$ and $LuGa_3$,[10] Therefore, specific heat measurement further supports that the KBi_2 is a type-I SC. On the other hand, the superconducting transition shifts to lower temperature with increasing field and the superconductivity is suppressed below 2.2 K when $H > 157$ Oe. In the normal state ($H = 307$ Oe), the electronic specific heat coefficient γ and phonon specific heat coefficient β are obtained using the linear fit $C_p/T = \gamma + \beta T^2$. The fitted γ and β is 1.3(4) mJ mol^{-1} K^{-2} and 3.10(4) mJ mol^{-1} K^{-4}, respectively. The latter one gives the Debye temperature $\Theta_D = 123.4(5)$ K using the formula $\Theta_D = (12\pi^4 NR/5\beta)^{1/3}$. The electron-phonon coupling λ_{e-ph} can be estimated with the values of Θ_D and T_c using McMillan's theory,[24]

$$\lambda_{e-ph} = \frac{1.04 + \mu^* \ln(\Theta_D/1.45T_c)}{(1 - 0.62\mu^*)\ln(\Theta_D/1.45T_c) - 1.04} \quad (1)$$

where μ^* is the repulsive screened Coulomb potential and is usually between 0.1 and 0.15. Setting $\mu^* = 0.13$, the calculated λ_{e-ph} is 0.774, implying that KBi_2 is an intermediately or strongly coupled BCS SC. Fig. 4(b) shows the specific heat of KBi_2 measured from 2.2 K to

300 K at zero field. The specific heat at high temperature approaches the value of $3NR$ at 300 K, where N is the atomic number in the chemical formula ($N = 3$) and R is the gas constant ($R = 8.314$ J mol^{-1} K^{-1}), consistent with the Dulong-Petit law. The electronic specific heat C_{es} at zero field (inset of Fig. 4(b)) is obtained by subtracting the lattice contribution from the total specific heat. The extracted electronic specific heat jump at T_c ($\Delta C_{es}/\gamma T_c = 6.06$) is much larger than the weakly coupled BCS value 1.43, indicating the strongly coupled superconductivity in KBi_2.[24]

The thermodynamic critical field $H_c(T)$ can be obtained by integrating the differences of specific heats and the specific heats divided by temperature between the zero-field superconducting (s) and normal (n) states ($H = 207$ Oe) (free energy analysis),[8,25]

$$-H_c(T)^2/8\pi = \Delta F(T) = \Delta U(T) - T\Delta S(T) \qquad (2)$$

$$\Delta U(T) = \int_T^{T_c} [C_s(T') - C_n(T')]dT' \qquad (3)$$

$$\Delta S(T) = \int_T^{T_c} \frac{C_s(T') - C_n(T')}{T'}dT' \qquad (4)$$

where $\Delta F(T)$, $\Delta U(T)$, and $\Delta S(T)$ are the differences of free energy, internal energy, and entropy between zero-field superconducting and normal states. The relationship between the T_c and critical fields determined from the magnetization, resistivity, specific heat measurements and free energy analysis is summarized in the $H - T$ phase diagram (Fig. 5). It can be seen that all of data are almost on one line, confirming the consistency of critical fields from different measuring methods and undoubtedly indicating that all of these critical fields are thermodynamic critical field $H_c(T)$. The dot line gives the free energy fitting that using the BCS temperature dependence $H_c(T) = H_c(0)[1 - (T/T_c)^2]$. This gives the zero-temperature $H_c(0) = 234.3(3)$ Oe and $T_c = 3.561(1)$ K, close to those values obtained from different experimental methods.

Fig. 6 shows the calculated density of state (DOS) of KBi_2. The shape of DOS is somewhat different from previous result,[15] because the SOC which is significant for bismuth is considered in present calculation. The finite DOS at Fermi energy level (E_F) indicates the metallic ground state, consistent with the experimental results. The DOS near E_F is mainly contributed by Bi-p state and the contribution of K is negligible, indicating that K atoms transfer almost all of valence electron to the Bi atoms, i.e. the valence state of K is +1 and the three-dimensional network of Bi can be thought as polyanion.[15]

The calculated total DOS at E_F is 1.77 states/eV-f.u. and it gives the carrier density $n = 6.33\times10^{22}$ cm^{-3} using the free-electron model. The calculated Fermi wave vector k_F equals 12.33 nm^{-1} using the formula

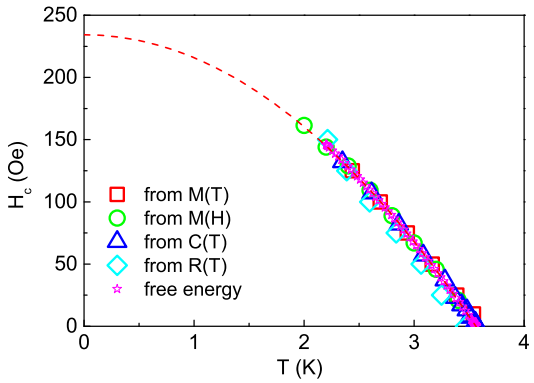

FIG. 5. $H - T$ phase diagram for KBi_2 determined from $M(T)$ (squares), $R(T)$ (triangles), and $C_p(T)$ (rhombuses) at various fields, $M(H)$ at various temperatures (circles) as well as that calculated from free energy analysis from zero-field specific heat data (stars). The dot line is fitted by using $H_c(T) = H_c(0)[1 - (T/T_c)^2]$.

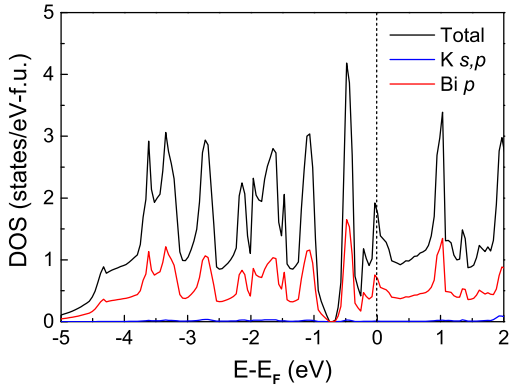

FIG. 6. Calculated density of states (DOS) of KBi_2. Black, red and blue lines correspond to the total DOS, partial DOS of Bi-p state and partial DOS of K-s,p state, respectively. The dotted line represents the Fermi energy level, E_F.

TABLE I. Physical parameters of KBi_2 in superconducting and normal states.

Parameter	Value
T_c (K)	3.573
H_c (Oe)	234.3(3)
RRR	72.5
γ (mJ/mol K^2)	1.3(4)
Θ_D (K)	123.4(5)
λ_{e-ph}	0.774
$\Delta C_{es}/\gamma T_c$	6.06
m* (m_e)	0.312
$\lambda_L(0)$ (nm)	11.8
l_{tr} (nm)	13.9
$\xi_{GL}(0)$ (nm)	133.7
$\lambda_{GL}(0)$ (nm)	81.7
κ_{GL}	0.611

$k_F = (3\pi^2 n)^{1/3}$. Then, the effective electron mass can be determined as $m^* = 3\hbar^2\gamma/(k_B^2 k_F V) = 0.312\ m_e$, where k_B is Boltzmann constant and m_e is the free electron mass. With derived m^* and n, the London penetration depth is calculated as $\lambda_L(0) = (m^*/\mu_0 n e^2)^{1/2} = 11.8$ nm.[26] Meanwhile the coherence length is determined by using the BCS relation $\xi(0) = 0.18\hbar^2 k_F/(k_B T_c m^*)$,[26] which gives $\xi(0) = 1.76\ \mu$m. Assuming a simple model of a spherical Fermi surface ($S/S_F = 1$), the mean free path l_{tr} is estimated as $l_{tr} = 1.27\times10^8(\rho_0 n^{2/3} S/S_F)^{-1} = 13.9$ nm, where ρ_0 is the low-temperature normal state resistivity (5.76 $\mu\Omega$ cm at 4 K).[26] It clearly indicates that the electronic mean free path is considerably smaller than the BCS coherence length ($l_{tr}/\xi(0) = 0.008$), suggesting that KBi_2 can be classified as a SC in the dirty limit. In the dirty limit, the GL parameter $\kappa_{GL} = 0.72\lambda_L(0)/l_{tr} = 0.611$,[26] which is smaller than $1/\sqrt{2}$, further confirming that KBi_2 is a type-I SC. Moreover, the zero-temperature Ginzburg-Landau (GL) coherence length in the dirty limit $\xi_{GL}(0)$ can be obtained from the relations $\xi_{GL}(0) = 8.57\times10^{-9}(10\gamma\rho_0 T_c/V)^{-1/2}$.[26] It gives $\xi_{GL}(0) = 133.7$ nm. According to the definition of $\kappa_{GL} = \lambda_{GL}(0)/\xi_{GL}(0)$, the derived zero-temperature GL penetration depth $\lambda_{GL}(0)$ is 81.7 nm. The superconducting and thermodynamic parameters of KBi_2 are summarized in Table I.

IV. CONCLUSION

In summary, the single crystal of KBi_2 has been grown from Bi flux successfully. Resistivity, magnetization and specific heat measurements indicate that KBi_2 shows a bulk superconductivity with $T_c = 3.573$ K. Further analysis of experimental results indicate that KBi_2 is type-I BCS SC in the dirty limit with an intermediate or strong coupling strength. The thermodynamic critical field is 234.3(3) Oe and the calculated GL parameter $\kappa_{GL} = 0.611$. This study not only deepens our understanding on type-I superconductivity but will also stimulate further work on discovering other type-I SCs in binary or ternary compounds.

V. ACKNOWLEDGMENTS

This work was supported by the Ministry of Science and Technology of China (973 Project: 2012CB921701), the Fundamental Research Funds for the Central Universities, and the Research Funds of Renmin University of China (RUC) (15XNLF06 and 14XNLQ03), and the National Natural Science Foundation of China (Grant No. 11574394). Computational resources have been provided by the PLHPC at RUC.

* hlei@ruc.edu.cn

[1] A. Abrikosov, Sov. Phys. JETP **5**, 1174 (1957).
[2] B. W. Roberts, J. Phys. Chem. Ref. Data **5**, 581 (1976).
[3] L. L. Zhao, S. Lausberg, H. Kim, M. A. Tanatar, M. Brando, R. Prozorov, and E. Morosan, Phys. Rev. B **85**, 214526 (2012).
[4] Y. Yamaguchi, S. Waki, and K. Mitsugi, J. Phys. Soc. Japan **56**, 419 (1987).
[5] U. Gottlieb, J. C. Lasjaunias, J. L. Tholence, O. Laborde, O. Thomas, and R. Madar, Phys. Rev. B **45**, 4803 (1992).
[6] G. W. Hull, J. H. Wernick, T. H. Geballe, J. V. Waszczak, and J. E. Bernardini, Phys. Rev. B **24**, 6715 (1981).
[7] T. T. M. Palstra, G. Lu, A. A. Menovsky, G. J. Nieuwenhuys, P. H. Kes, and J. A. Mydosh , Phys. Rev. B **34**, 4566 (1986).
[8] V. K. Anand, A. D. Hillier, D. T. Adroja, A. M. Strydom, H. Michor, K. A. McEwen, and B. D. Rainford, Phys. Rev. B **83**, 064522 (2011).
[9] S. Yonezawa and Y. Maeno, Phys. Rev. B **72**, 180504(R) (2005).
[10] E. Svanidze and E. Morosan, Phys. Rev. B **85**, 174514 (2012).
[11] J. M. Reynolds and C. T. Lane, Phys. Rev. **79**, 405 (1950).
[12] B. T. Matthias and J. K. Hulm, Phys. Rev **87**, 799 (1952).
[13] X. Zhang, H. C. Lei, and C. Petrovic, Phys. Rev. B **86**, 054502 (2012).
[14] K. Nishimura, T. Yasukawa, and K. Mori, Phys. B **329-333**, 1399 (2003).
[15] S. Ponou, N. Müller, T. F. Fässler, and U. Häussermann, Inorg. Chem. **44**, 7423 (2005).
[16] TOPAS Version 4; Bruker AXS, Karlsruhe, Germany, 2007.
[17] P. E. Blöchl, Phys. Rev. B **50**, 17953 (1994); G. Kresse and D. Joubert, *ibid.* **59**, 1758 (1999).
[18] G. Kresse and J. Hafner, Phys. Rev. B **47**, 558 (1993); G. Kresse and J. Furthmüller, Comp. Mater. Sci. **6**, 15 (1996); Phys. Rev. B **54**, 11169 (1996).
[19] J. P. Perdew, K. Burke, and M. Ernzerhof, Phys. Rev. Lett. **77**, 3865 (1996).
[20] F. Emmerling, N. Längin, D. Petri, M. Kroeker, and C. Röhr, Z. Anorg. Allg. Chem. **630**, 171 (2004).
[21] A. N. Kuznetsov and T. F. Fässler, Z. Anorg. Allg. Chem. **628**, 2537 (2002).
[22] A. Aharoni, J. Appli. Phys. **83**, 3432 (1998).
[23] V. H. Tran, Z. Bukowski, P. Wisniewski, L. M. Tran, and A. J. Zaleski, J. Phys.: Condens. Matter **25**, 155701 (2013).
[24] W. L. McMillan, Phys. Rev. **167**, 331 (1968).
[25] Y. Wang, R. Lortz, Y. Paderno, V. Filippov, S. Abe, U. Tutsch, and A. Junod, Phys. Rev. B **72**, 024548 (2005).
[26] T. P. Orlando, E. J. McNiff, Jr., S. Foner, and M. R. Beasley, Phys. Rev. B **19**, 4545 (1979).